This article has been accepted for publication in a future issue of this journal, but has not been fully edited. Content may change prior to final publication. Citation information: DOI 10.1109/ACCESS.2021.3117363, IEEE Access

IEEE Access
Multidisciplinary | Rapid Review | Open Access Journal

Date of publication xxxx 00, 0000, date of current version xxxx 00, 0000.

Digital Object Identifier 10.1109/ACCESS.2017.DOI

Backstepping Nonsingular Terminal Sliding Mode Control for PMSM with Finite-time Disturbance Observer

TONG LI[1] XUDONG LIU[1,2], AND HAISHENG YU[1]

[1]College of Automation and Electrical Engineering, Qingdao University, Qingdao 266071, China
[2]Shandong Key Laboratory of Industrial Control Technology, Qingdao 266071, China

Corresponding author: Xudong Liu (e-mail: xudong19871982@163.com).

This work was supported by the National Natural Science Foundation of China under Grant No. 61703222, in part by the China Postdoctoral Science Foundation under Grant No.2018M632622, in part by the Science and Technology Support Plan for Youth Innovation of Universities in Shandong Province under Grant No. 2019KJN033.

ABSTRACT Aiming at the speed regulation problem of permanent magnet synchronous motor (PMSM) drives, a novel backstepping nonsingular terminal sliding mode control (BNTSMC) method with finite-time disturbance observer (FTDO) is proposed. In order to ensure excellent tracking and anti-disturbance performance, the backstepping nonsingular terminal sliding mode speed controller based on equivalent motor model and the recursive principle is designed for PMSM. The benefits of this approach are that the controller has asymptotic stability based on backstepping design, finite-time convergence, and strong robustness for the matched disturbance based on sliding mode control. Then, to further improve the anti-disturbance performance, a finite-time disturbance observer is designed, and it is used to estimate the mismatched external disturbance in motor drive system. The stability of the system is also proved with Lyapunov criterion. Finally, the experimental results show that the proposed method has the advantages of fast convergence and strong robustness against parameter variations and external disturbance.

INDEX TERMS PMSM drive, backstepping nonsingular terminal sliding mode control (BNTSMC), finite-time disturbance observer (FTDO).

I. INTRODUCTION

At present, induction motor (IM) and permanent magnet synchronous motor (PMSM) are widely used in the industrial applications, and they occupy the vast majority of the market share. Meanwhile, switched reluctance motor (SRM) is also in the rapid development, but due to the problems of high noise and low-speed torque ripple, it still has few applications. Compared with IM, PMSM has the advantages of simple structure, high efficiency, high power density, and low noise [1]. To realize the high performance control of PMSM, the field oriented control is popular used in the motor drives [2], and the double closed loop speed controller is constructed by using PI control method. However, due to the strong external disturbance and model uncertainty in complex working conditions, the PI controller cannot meet the practical requirements for some high performance applications. With the development of control theory and microcomputer technology, the nonlinear control strategies have been applied to PMSM drives, such as sliding model control [3-4], model predictive control [5], backstepping control [6], active disturbance rejection control [7], repetitive learning control [8], and intelligent control [9].

Among these methods, backstepping control, as a nonlinear recursive design method, is proposed in 1990s [10]. This method is based on Lyapunov stability theory, the control law is derived by constructing the Lyapunov function, and the global asymptotic stability is ensured [11]. For the motor drive system, the complex nonlinear electromechanical control system can be decomposed into several subsystems by using the backstepping control method. The servo or speed controller of the motor can be realized by recursive design and introducing virtual control variables [12]. In [13], a full adaptive backstepping speed control method is proposed by estimating the all motor parameters and external disturbance, and the fast tracking and robustness performance is ensured, but the method is complex. In [14], an offset-free robust backstepping method is proposed for PMSM, and the novel adaptive law by using multivariable approach is designed

This work is licensed under a Creative Commons Attribution-NonCommercial-NoDerivatives 4.0 License. For more information, see https://creativecommons.org/licenses/by-nc-nd/4.0/

This article has been accepted for publication in a future issue of this journal, but has not been fully edited. Content may change prior to final publication. Citation information: DOI 10.1109/ACCESS.2021.3117363, IEEE Access

to improve the robustness. By using maximum torque per ampere and flux-weakening control, the control laws for the entire speed range of PMSM are developed based on an adaptive backstepping technique in [15]. In [16], a backstepping control method based on a new load torque update law is proposed for the servo control of PMSM, and the servo tracking performance is improved effectively. In [17], a discontinuous projection-based robust backstepping controller is proposed for the high-accuracy speed control of PMSM for wind turbines, and an extended state observer is designed to handle the disturbance. In [18], a composite controller based on backstepping control and linear extended state observer is designed, and the robustness for time-varying parameter disturbance is considered in the paper.

However, backstepping control is a strict model-based control method, thus the single backstepping controller cannot ensure the robustness of PMSM drives under complex working condition. To improve the anti-disturbance performance, the adaptive backstepping controller by using adaptive laws are designed in [13-17], but the convergence speed with the unknown parameters and the external disturbance to the true values is always a concern, which may lead to slow convergence [19]. By combining neural network and backstepping control, the servo tracking controller for PMSM is designed to satisfy the robustness of the system [20].

As is known, sliding mode control (SMC) has been proved to be a potentially useful approach in industrial applications, such as actuator [21], robot [22-23] and PMSM [3-4]. Many advanced sliding mode control methods are widely used in motor drive, such as fractional order sliding mode control [24], terminal sliding mode control [25] and integral sliding mode control [26]. The integral sliding mode control has the advantage of fast convergence, however, the relationship between response speed and chattering needs to be weighed in parameter selection, and the disturbance observer can effectively solve this problem [27]. The nonsingular terminal sliding mode has the advantages of finite time convergence, good tracking performance and strong robustness, which has attracted great attention. By combining the advantages of backstepping control and sliding mode control, it can be an effective method to improve the system performance [28-29]. The composite approach preserves the merits of the sliding mode control in terms of high robustness and fast transient response, as well as backstepping control strategy in terms of globally asymptotic stability based on Lyapunov criterion, and it has been used in some applications, such as, robot manipulators [11], new energy power generation system [30], automotive vehicle [31]. In [6], a non-cascade backstepping sliding mode control strategy is proposed for PMSM drives, and the sliding mode control is used to improve the anti-disturbance for the parameter disturbance. Although sliding mode control is less sensitive to disturbance, it is noticed that the common SMC only has the robustness to the matched disturbance, which means the uncertainties exist in the same channel as that of the control input [32]. For the motor drive system, the mismatched disturbance (such as the external load torque) exists when the single-loop controller is designed for the speed control [33]. On the other hand, through the improved sliding mode method, the mismatched disturbance can be suppressed, but a large sliding mode switching gain is needed for the strong mismatched disturbance, the chatting will be increased, and the control performance will be influenced. In order to reduce the chattering, some improved sliding mode control methods are used in the control system, such as boundary layer control [34-36] and full-order sliding mode control [37]. Recently, the disturbance estimation and attenuation methods [38], such as, disturbance observer [32, 39], extended state observer [40], sliding mode observer [41] and finite-time disturbance observer [42], have been proposed to deal with the disturbance, which includes the matched and mismatched disturbance. In [17-18, 43-45], the composite control strategies with backstepping control and disturbance attenuation technologies are designed for PMSM, and the estimated disturbance is used for the feed-forward compensation control, the anti-disturbance ability can be improved. Meanwhile, the dynamic performance is almost unaffected.

In this paper, to improve the speed regulation performance of PMSM, a novel backstepping sliding mode control strategy based on finite-time disturbance observer (FTDO) is proposed. The main contributions of this paper are

(1) By combining the advantages of backstepping control with asymptotic stability and nonsingular terminal sliding mode control (BNTSMC) with finite-time convergence, and strong robustness for the matched disturbance, a novel single-loop non-cascade controller is designed for PMSM, which effectively simplifies the controller structure.

(2) Although the designed controller has the robustness for the electromagnetic parameter disturbance, it cannot suppress the mismatched external disturbance effectively. Thus, a finite-time disturbance observer is designed to the single-loop non-cascade control of PMSM, and it is used to estimate the external load disturbance.

(3) The proposed method is compared with conventional PI control, backstepping control with disturbance observer. The comparative experimental results show that the proposed method has the good transient performance and the strong robustness for the load and parameter disturbance.

This paper is organized as follows. In Section II, the mathematical model of PMSM is established. The speed controller basedon BNTSMC and finite-time disturbance observer is discussed in Section III. Experimental results and analysis are demonstrated in Section IV, which is followed by conclusion in Section V.

II. MATHEMATICAL MODEL OF PMSM

According to the field oriented control principle, in the case of neglecting the iron loss, the current dynamic model of PMSM in d-q synchronous reference frame can be written

This work is licensed under a Creative Commons Attribution-NonCommercial-NoDerivatives 4.0 License. For more information, see https://creativecommons.org/licenses/by-nc-nd/4.0/

This article has been accepted for publication in a future issue of this journal, but has not been fully edited. Content may change prior to final publication. Citation information: DOI 10.1109/ACCESS.2021.3117363, IEEE Access

as [46-47]

$$\begin{cases} \frac{di_d}{dt} = \frac{-R_s i_d}{L_d} + n_p\omega\frac{L_q}{L_d}i_q + \frac{1}{L_d}u_d \\ \frac{di_q}{dt} = \frac{-R_s i_q}{L_q} - \frac{n_p\omega L_d i_d}{L_q} - \frac{n_p\omega\Phi}{L_q} + \frac{1}{L_q}u_q \end{cases} \tag{1}$$

And the motion equation can be described as

$$\frac{d\omega}{dt} = \frac{T_e}{J} - \frac{T_L}{J} - \frac{B}{J}\omega \tag{2}$$

The electromagnetic torque in d-q synchronous reference frame is

$$T_e = n_p\Phi i_q \tag{3}$$

where L_d and L_q represent d-axes and q-axes stator inductances, respectively, i_d and i_q are the stator current, u_d and u_q are the stator input voltage in dq-axes reference frame, R_s is the per-phase stator resistance, n_p is the number of pole pairs, ω is the mechanical angular speed of the rotor, Φ is the rotor flux, J is the moment of inertia, T_e is the electromagnetic torque, T_L is the load torque, B is the viscous friction coefficient.

A surface mounted PMSM (SPMSM) is discussed in this paper, and the d-axes inductance can be considered equal to q-axes inductance, $L_d = L_q$. Thus, the electromagnetic torque can be rewritten as $T_e = n_p\Phi i_q$, from (2), the motion equation is

$$\frac{d\omega}{dt} = \frac{n_p\Phi i_q}{J} - \frac{T_L}{J} - \frac{B}{J}\omega \tag{4}$$

In the conventional speed drive control of PMSM, the cascade control structure with the inner current loop and the outer speed loop is usually adopted as shown in Fig.1, and the PI control method is used for the speed loop and current loop. For the SPMSM, the d-axes reference current i_d^* is set to zero to ensure a constant flux operating condition. ω^* is the reference speed. In order to improve the speed control performance, a backstepping nonsingular terminal sliding mode control strategy with finite-time disturbance observer is proposed in this paper, and it is used to replace the PI control. The control structure with the proposed method is shown in Fig.2.

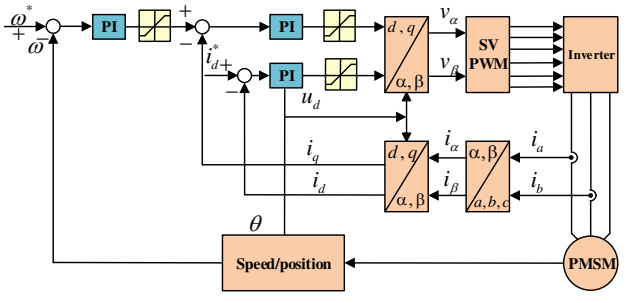

FIGURE 1: The control system of PMSM speed drive system with PI controller.

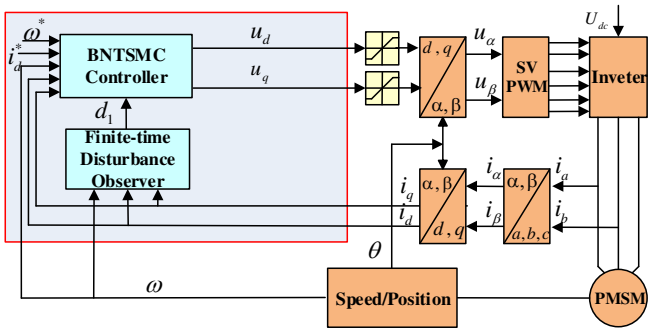

FIGURE 2: The control structure of PMSM speed drive system with the proposed method.

III. DESIGN OF SPEED CONTROLLER WITH BNTSMC AND FTDO

In this paper, a novel speed control method is proposed to improve the speed control performance of PMSM drives. The design process includes q-axes controller and d-axes current controller, and they will be designed with backstepping nonsingular terminal sliding mode control. In addition, to suppress the mismatched disturbance, the finite-time disturbance observer is designed. The previous NTSMC control is mostly used in cascade control, while the NTSMC control proposed in this paper adopts non-cascade control method, which effectively simplifies the system structure. Finally, the experimental results show that the proposed method has good control performance.

A. DESIGN OF Q-AXES CONTROLLER

Firstly, define the variables $x_1 = \omega$ and $x_2 = \frac{n_p\Phi}{J}i_q$. From (1) and (4), the second-order system can be derived as follows, which is convenient for the design of controller.

$$\begin{cases} \dot{x}_1 = x_2 + d_1 \\ \dot{x}_2 = f(x) + bu \end{cases} \tag{5}$$

where $f(x) = \frac{n_p\Phi}{J}(-\frac{R_s i_q}{L_q} - \frac{n_p\omega L_d i_d}{L_q} - \frac{n_p\omega\Phi}{L_q})$, $b = \frac{n_p\Phi}{JL_q}$ is the input coefficient. $u = u_q$ is the nonsingular terminal sliding mode control input. $d_1 = -\frac{T_L}{J} - \frac{B}{J}\omega$ is the lump disturbance, and it can also be defined as the mismatched disturbance.

Define the motor reference speed as $x_1^* = \omega^*$, then the speed tracking error between the actual speed and reference speed is $e_1 = x_1 - x_1^*$. Backstepping control is completed based on Lyapunov stability theory, and the control law is derived by constructing the Lyapunov function. Taking a Lyapunov candidate function as $V_1 = \frac{1}{2}e_1^2$, then differentiating V_1 with respect to time as

$$\begin{aligned} \dot{V}_1 &= e_1\dot{e}_1 = e_1(\dot{x}_1 - \dot{x}_1^*) = e_1(x_2 + d_1 - \dot{x}_1^*) \\ &= e_1(x_2 + d_1 - \dot{x}_1^* - c_1e_1 + c_1e_1) \end{aligned} \tag{6}$$

From (6), a virtual control input is chosen as $x_2^* = \dot{x}_1^* - d_1 - c_1e_1$, and $\dot{V}_1 = -c_1e_1^2 \leq 0$ can be obtained. Consequently, e_1 will be asymptotically convergence. Then,

This work is licensed under a Creative Commons Attribution-NonCommercial-NoDerivatives 4.0 License. For more information, see https://creativecommons.org/licenses/by-nc-nd/4.0/

This article has been accepted for publication in a future issue of this journal, but has not been fully edited. Content may change prior to final publication. Citation information: DOI 10.1109/ACCESS.2021.3117363, IEEE Access

according to the recursive principle, the second error variable is defined as $e_2 = x_2 - x_2^*$, $e_2(0) = x_2(0) - x_2^*(0)$, differentiating e_2 with respect to time is

$$\begin{aligned}\dot{e}_2 &= \dot{x}_2 - \dot{x}_2^* = f(x) + bu - \dot{x}_2^* \\ &= f(x) + bu - \ddot{x}_1^* + \dot{d}_1 + c_1\dot{e}_1 \\ &= f(x) + bu - \ddot{x}_1^* + \dot{d}_1 + c_1(x_2 + d_1 - \dot{x}_1^*)\end{aligned} \tag{7}$$

By using nonsingular terminal sliding mode control method, and the process can be divided into two parts, one is the design of the sliding mode surface and the other is approach law. Firstly, the nonsingular terminal sliding mode surface is chosen as

$$s_1 = e_2 + \beta_1 \int {e_2}^{p_1/q_1} \tag{8}$$

where $\beta_1 > 0$, p_1 and q_1 are positive odd integers, and $1 < p_1/q_1 < 2$.

According to reference [26], on the sliding mode surface $s_1 = 0$, the derivation of equation (8) can be expressed as

$$\dot{e}_2 = -\beta_1 {e_2}^{p_1/q_1} \tag{9}$$

By solving the error dynamic equation (9), the convergence time of T_{f_1} is obtained as follows:

$$T_{f_1} = \frac{|e_2(0)|^{1-p_1/q_1}}{\beta_1(1 - p_1/q_1)} \tag{10}$$

It is proved that the sliding mode surface converges in finite time T_{f_1}.

Take the first derivative of s_1 as

$$\dot{s}_1 = \dot{e}_2 + \beta_1 {e_2}^{p_1/q_1} \tag{11}$$

Select the exponential approach law of sliding mode control as

$$\dot{s}_1 = -k_1 sgn(s_1) - k_2 s_1 \tag{12}$$

where k_1, k_2, are sliding mode control gains.

From (7), (11) and (12), the q-axes current controller can be derived as

$$\begin{aligned}u_q = u = -\tfrac{1}{b}\left[f(x) - \ddot{x}_1^* + \dot{d}_1 + c_1(x_2 + d_1 - \dot{x}_1^*)\right] \\ -\tfrac{1}{b}\left[\beta_1 {e_2}^{p_1/q_1} + k_1 sgn(s_1) + k_2 s_1\right]\end{aligned} \tag{13}$$

Considering the follow Lyapunov function $V_2 = V_1 + \frac{1}{2}{s_1}^2$, then $\dot{V}_2 \le -c_1 e_1^2 - k_2 s_1^2 - k_1 |s_1| \le 0$. Therefore, the control system with the proposed backstepping nonsingular terminal sliding mode controller is asymptotically stable. From the control law (13), the disturbance information exists in the designed controller. Although sliding mode control has good robustness for the matched disturbance, the mismatched disturbance existed in motor model (5) cannot be suppressed through the sliding mode control [32]. An alternative solution to the disturbance is to make the control law adaptive to the disturbance, which is estimated online by an observer [38]. And it will be introduced in C.

B. DESIGN OF D-AXES CURRENT CONTROLLER

Define the d-axes current tracking error as $e_3 = i_d - i_d^*$, $e_3(0) = i_d(0) - i_d^*(0)$. i_d^* is the d-axes reference current. To ensure a constant flux, $i_d^* = 0$ is chosen. Similarly, take the first derivative of e_3 as

$$\dot{e}_3 = \dot{i}_d - \dot{i}_d^* = \frac{-R_s i_d}{L_d} + n_p\omega\frac{L_q}{L_d}i_q + \frac{1}{L_d}u_d \tag{14}$$

The design of d-axes is mainly realized by nonsingular terminal sliding mode control, and its sliding surface is designed as follows

$$s_2 = e_3 + \beta_2 \int {e_3}^{p_2/q_2} \tag{15}$$

The sliding mode approximation approach law is chosen as

$$\dot{s}_2 = -k_3 sgn(s_2) - k_4 s_2 \tag{16}$$

In order to ensure the nonsingular and fast convergence of the sliding mode control, the parameters are selected as follows. Where $\beta_2 > 0$, p_2 and q_2 are positive odd integers, $1 < p_2/q_2 < 2$, $k_3 > 0$, $k_4 > 0$.

Then, the derivation of equation (15) can be expressed as

$$\dot{s}_2 = \dot{e}_3 + \beta_2 {e_3}^{p_2/q_2} \tag{17}$$

According to (14), (16) and (17), d-axes current control input is derived as

$$u_d = L_d\left[\frac{R_s i_d}{L_d} - n_p\omega\frac{L_q}{L_d}i_q - \beta_2 {e_3}^{p_2/q_2} - k_3 sgn(s_2) - k_4 s_2\right] \tag{18}$$

Choose a Lyapunov function as $V_3 = \frac{1}{2}{s_2}^2$, and $\dot{V}_3 = s_2\dot{s}_2 = -k_4{s_2}^2 - k_3|s_2| \le 0$ can be guaranteed. Thus, the d-axes current will converge to zero. During the operation of the motor, the influence of external factors such as temperature leads to the change of electromagnetic parameters, and these variations can be regarded as the matched disturbance. By using the good robustness for matched disturbance of sliding mode control, the excellent current control performance can be obtained.

C. DESIGN OF FINITE-TIME DISTURBANCE OBSERVER

For the actual motor drive system, the load torque disturbance is inevitable. As seen in (13), the mismatched disturbance d_1 exists in the q-axes current controller. If the disturbance is ignored, the control performance will be influenced. Sliding mode control has strong robustness to the matched disturbance in motor operation, but it is not effective to suppress the mismatched disturbance caused by the change of load torque in the single-loop controller. Therefore, to improve the anti-disturbance performance of the controller, a finite-time disturbance observer [48-49] is designed for PMSM control system, and it is used to estimate the mismatched disturbance d_1. The disturbance observer is designed as follows.

Lemmas1: [50] Consider the following system:

This work is licensed under a Creative Commons Attribution-NonCommercial-NoDerivatives 4.0 License. For more information, see https://creativecommons.org/licenses/by-nc-nd/4.0/

This article has been accepted for publication in a future issue of this journal, but has not been fully edited. Content may change prior to final publication. Citation information: DOI 10.1109/ACCESS.2021.3117363, IEEE Access

$$\begin{aligned}
&\dot{\delta}_0 = -\lambda_0|\delta_0|^{n/(n+1)}sign(\delta_0) - \vartheta_0\delta_0 + \delta_1\\
&\dot{\delta}_1 = -\lambda_1\left|\delta_1 - \dot{\delta}_0\right|^{(n-1)/n}sign(\delta_1 - \dot{\delta}_0) - \vartheta_1(\delta_1 - \dot{\delta}_0) + \delta_2\\
&\vdots\\
&\dot{\delta}_{n-1} = -\lambda_{n-1}\left|\delta_{n-1} - \dot{\delta}_{n-2}\right|^{1/2}sign(\delta_{n-1} - \dot{\delta}_{n-2})\\
&-\vartheta_{n-1}(\delta_{n-1} - \dot{\delta}_{n-2}) + \delta_n\\
&\dot{\delta}_n = -\lambda_n sign(\delta_n - \dot{\delta}_{n-1}) - \vartheta_n(\delta_n - \dot{\delta}_{n-1}) - \tfrac{1}{L_0}f(t)
\end{aligned} \tag{19}$$

where $\delta_0, \cdots, \delta_n$ are the scalar state variables, $\lambda_0, \cdots, \lambda_n$ and $\vartheta_0, \cdots, \vartheta_n$ are appropriate positive constants, L_0 is a proper positive constant, and the perturbation term $f(t)$ satisfies $|f(t)| \leq L_0$. Then, the system converges to the origin in finite time, i.e., it is finite-time stable.

$$\begin{cases}
\dot{z}_0 = v_0 + x_2\\
v_0 = -\lambda_0 {L_1}^{1/3}|z_0 - x_1|^{2/3}sgn(z_0 - x_1) + z_1\\
\dot{z}_1 = v_1\\
v_1 = -\lambda_1 {L_1}^{1/2}|z_1 - v_0|^{1/2}sgn(z_1 - v_0) + z_2\\
\dot{z}_2 = -\lambda_2 L_1 sgn(z_2 - v_1)
\end{cases} \tag{20}$$

where z_0 is the estimation of x_1. z_1 is the estimate of d_1. z_2 is the estimate of $\dot{d}_1$. λ_0, λ_1 and λ_2 are the positive observer coefficients to designed. L_1 is proper positive Lipschitz constant.

Then, let $e_{x_1} = z_0 - x_1$, $e_{d_1} = z_1 - d_1$, $e_{\dot{d}_1} = z_2 - \dot{d}_1$. Differentiate the time of e_{x_1}, e_{d_1}, and $e_{\dot{d}_1}$ respectively, and we can obtain

$$\begin{aligned}
\dot{e}_{x_1} &= \dot{z}_0 - \dot{x}_1\\
&= -\lambda_0 {L_1}^{1/3}|e_{x_1}|^{2/3}sgn(e_{x_1}) + e_{d_1}
\end{aligned} \tag{21}$$

$$\begin{aligned}
\dot{e}_{d_1} &= \dot{z}_1 - \dot{d}_1\\
&= -\lambda_1 {L_1}^{1/2}|e_{d_1} - \dot{e}_{x_1}|^{1/2}sgn(e_{d_1} - \dot{e}_{x_1}) + e_{\dot{d}_1}
\end{aligned} \tag{22}$$

$$\dot{e}_{\dot{d}_1} \in -\lambda_2 L_1 sgn(e_{\dot{d}_1} - \dot{e}_{d_1}) + [-L_1, L_1] \tag{23}$$

Assume the load torque disturbance changes slowly, d_1 is bounded, according to Lemmas1, the estimation value will converge to the actual value in finite time [51].

Through the finite-time disturbance observer, the disturbance d_1 is estimated effectively, and it is used in the controller (13) for the compensation of the disturbance. The finite-time disturbance observer solves the problem that the sliding mode control cannot deal with the mismatched disturbance, and the robustness of the drive system is improved.

To sum up, by combining the designed backstepping terminal sliding mode control laws (13), (18) and the finite-time disturbance observer (20), the reference voltage signals can be derived.

D. PROOF OF THE SYSTEM STABILITY

Through the design of d-axes current controller, it can be seen that the d-axes control system is stable. For the design of q-axes controller, considering the motor model (5) with the disturbance, when the FTDO selects the appropriate parameters, a composite control combining FTDO and BNTSMC can be obtained. The control rate u_q can be expressed as

$$\begin{aligned}
u_q = u = &-\tfrac{1}{b}\left[f(x) - \ddot{x}_1^* + \hat{\dot{d}}_1 + c_1(x_2 + \hat{d}_1 - \dot{x}_1^*)\right]\\
&-\tfrac{1}{b}\left[\beta_1 e_2^{p_1/q_1} + k_1 sgn(s_1) + k_2 s_1\right]
\end{aligned} \tag{24}$$

Define the Lyapunov function $V = V_2 + V_3$. According to the previous definition of $V_2 = V_1 + \frac{1}{2}s_1^2$, taking the derivative of V and combining (7), (11), (12), (14), (17), (18) and the control rate (24), $\dot{V}$ can be expressed as

$$\begin{aligned}
\dot{V} &= \dot{V}_2 + \dot{V}_3\\
&= \dot{V}_1 + \dot{s}_1 s_1 + \dot{V}_3\\
&= -c_1 e_1^2 + s_1(\dot{e}_2 + \beta_1 e_2^{p_1/p_2}) + \dot{s}_2 s_2\\
&= -c_1 e_1^2 + s_1(f(x) + bu - \ddot{x}_1^* + \dot{d}_1 + c_1(x_2 + d_1 - \dot{x}_1^*)\\
&+\beta_1 e_2^{p_1/p_2}) - k_3|s_2| - k_4 s_2^2\\
&= -c_1 e_1^2 - s_1(\hat{\dot{d}}_1 - \dot{d}_1 + c_1(\hat{d}_1 - d_1) + k_1 sgn(s_1) + k_2 s_1)\\
&-k_3|s_2| - k_4 s_2^2\\
&= -c_1 e_1^2 - s_1(e_{\dot{d}_1} + c_1 e_{d_1} + k_1 sgn(s_1) + k_2 s_1)\\
&-k_3|s_2| - k_4 s_2^2\\
&= -c_1 e_1^2 - s_1(e_{\dot{d}_1} + c_1 e_{d_1}) - k_1|s_1| - k_2 s_1^2 - k_3|s_2| - k_4 s_2^2
\end{aligned} \tag{25}$$

It is assumed that $\left|(\hat{d}_1 - d_1) = e_{d_1}\right| \leq D_1$, $\left|(\hat{\dot{d}}_1 - \dot{d}_1) = e_{\dot{d}_1}\right| \leq D_{11}$, and D_1, D_{11}, are positive, and $\dot{d}$ is inherently bounded. The equation (25) is simplified to

$$\begin{aligned}
\dot{V} &\leq -c_1 e_1^2 - k_1|s_1| + (D_{11} + c_1 D_1)|s_1|\\
&-k_2 s_1^2 - k_3|s_2| - k_4 s_2^2\\
&= -c_1 e_1^2 - (k_1 - D_{11} - c_1 D_1)|s_1| - k_2 s_1^2 - k_3|s_2| - k_4 s_2^2
\end{aligned} \tag{26}$$

When the choice of k_1 satisfies $k_1 - D_{11} + c_1 D_1 \geq 0$, and $\dot{V} \leq 0$. Thus, the asymptotical stability of the system is proved.

IV. EXPERIMENT RESULTS AND ANALYSIS

To verify the effectiveness of the proposed backstepping nonsingular terminal sliding mode control with finite-time disturbance observer (BNTSMC+FTDO), a 130MB150A nonsalient permanent magnet synchronous motor drive system is taken as an example to conduct experiments. The experimental platform is shown in Fig.3. The structure diagram of the speed control experiment of the drive system is shown in Fig.4. The sampling frequency of the IGBT is 10kHz. The fundamental sample time of Simulink is 0.1ms. The sampling period of the current loop is 0.1ms, and the sampling period of the speed loop is 10ms. When the control algorithm is compiled into the target code, it is downloaded to the target computer to run through the RT-SIM software. The target machine controls the motor through a special control

This work is licensed under a Creative Commons Attribution-NonCommercial-NoDerivatives 4.0 License. For more information, see https://creativecommons.org/licenses/by-nc-nd/4.0/

This article has been accepted for publication in a future issue of this journal, but has not been fully edited. Content may change prior to final publication. Citation information: DOI 10.1109/ACCESS.2021.3117363, IEEE Access

TABLE 1: Parameters of Motor

Description	Value	Unit
rated speed	1000	r/min
rated power	1.5	kW
moment of inertia	0.0027	$kg \cdot m^2$
permanent magnet flux	0.32	Wb
line resistance	1.84	Ω
line inductance	6.65	mH
number of pole pairs	4	

card. In addition, the Links-RT real-time simulation software package can record and monitor the experimental data in real time, which can facilitate real-time verification of the control performance of the proposed method. The motor parameters are shown in Table 1.

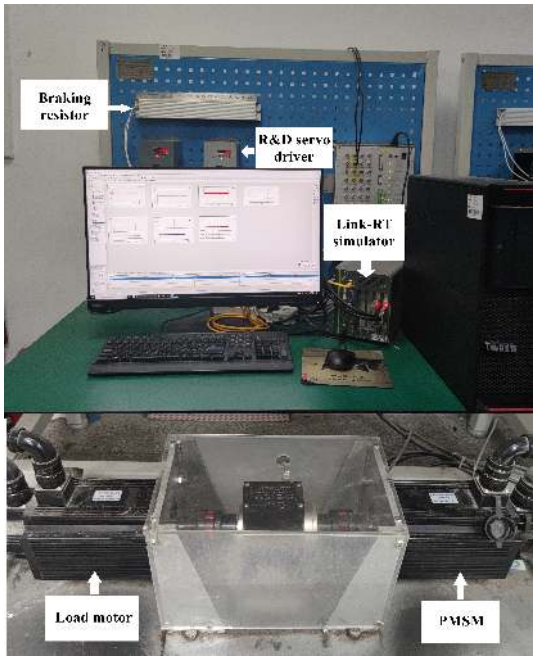

FIGURE 3: Experiment platform.

In order to better verify the effectiveness, the proposed method is compared with the PI controller, backstepping controller with nonlinear disturbance observer (BC+NDO) in this section. In terms of PI controller, the parameters of the speed loop are $K_p = 0.04$, $K_i = 0.5$, and the two current loops are selected for the same parameters as $K_p = 9$, $K_i = 100$. In the parameter selection of BNTSMC+FTDO, the choice of c_1 in the controller affects the convergence rate of the system, β_1 and β_2 have a greater impact on the chattering of the system. Similar in the sliding mode gain, the choice of k_1 and k_3 has a greater impact on the chattering of the system, while the choice of k_2 and k_4 affects the convergence of the sliding mode surface. In order to reduce chattering, β_1, β_2, k_1, k_3 are selected with smaller parameters. The larger sliding mode gain k_2, k_4 and controller parameter c_1 are

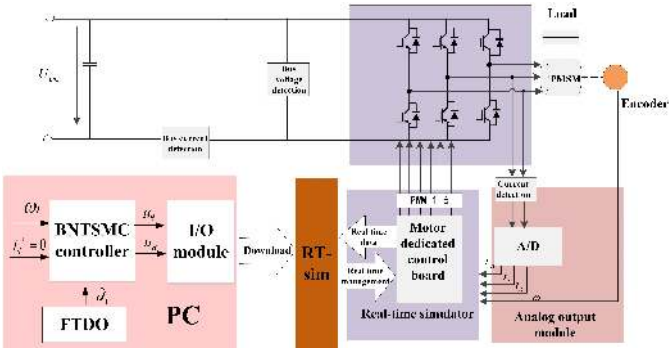

FIGURE 4: The configuration of the experimental PMSM drive system.

selected to ensure the faster convergence. However, excessive selection of the above parameters will cause large overshoot. In order to alleviate the above problems, the parameters of the observer can alleviate the problem of excessive parameter selection of the controller to a certain extent. At the same time, the larger parameters of the observer can reduce the speed drop and accelerate the recovery time. In order to balance the fast convergence, speed overshoot and chattering, the parameters are obtained by trial and error method. We get the following parameters $c_1 = 500$, $\beta_1 = 2$, β_2=10, $p_1 = 7$, $q_1 = 5$, $p_2 = 7$, $q_2 = 5$, $k_1 = 10$, $k_2 = 1200$, $k_3 = 50$, $k_4 = 1800$, $L_1 = 20$, $\lambda_0 = \lambda_1 = \lambda_2 = 50$. The system has obtained fascinating control effect through the final parameter selection.

In order to ensure the fairness of comparison, in these three methods, the response speed, overshoot and anti-disturbance performance are comprehensively considered. The controller parameters are adjusted repeatedly, and the trial and error method is used to ensure the best control performance of the system. In addition, in the experiment, the comparison of the experiment is completed under the same conditions.

In the experiment, the performance of the control method has been studied with 200r/min, 600r/min, and 1000r/min as the reference speeds. The motor starts with a load torque of $0.5N \cdot m$. The speed response curves of PI, BC+NDO,NTSMC+DO, BNTSMC, and BNTSMC+FTDO are shown in Fig.5. It can be seen from the Fig.5 that the overshoots of PI and BC+NDO control methods at 200r/min, 600r/min, and 1000r/min are 28r, 48r, 81r, and 14r, 22r, 41r, respectively. And the response time is 0.50s, 0.56s, 0.58s and 0.27s, 0.31s, 0.36s, respectively. And the overshoot and response time of the NTSMC+DO control method are 17r, 21r, 29r, and 0.29s, 0.50s, 0.52s, respectively. The overshoot and response time of the proposed BNTSMC+FTDO method are 13r, 6r, 10r, and 0.25s, 0.27s, 0.28s, respectively. The control precision at 200r/min is $\pm 6r$, and the relative control precision is 3%. The control precision at 600r/min is ± 2, and the relative control precision is 0.33%. Similarly, the control precision at 1000r/min is ± 3, and the relative control precision is 0.3%. Through the comparison of experimental

This work is licensed under a Creative Commons Attribution-NonCommercial-NoDerivatives 4.0 License. For more information, see https://creativecommons.org/licenses/by-nc-nd/4.0/

This article has been accepted for publication in a future issue of this journal, but has not been fully edited. Content may change prior to final publication. Citation information: DOI 10.1109/ACCESS.2021.3117363, IEEE Access

data, because the motor starts with $0.5N \cdot m$ load, it is difficult for BNTSMC method to reach the rated speed. The finite-time disturbance observer estimates the load torque disturbance effectively and the estimated disturbance is used for the feed-forward compensation control. It is shown that BNTSMC+FTDO control method has small overshoot and fast response.

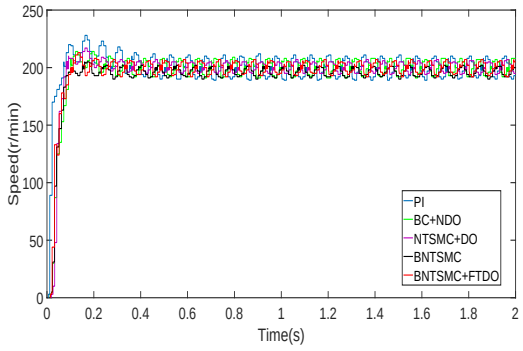

(a)

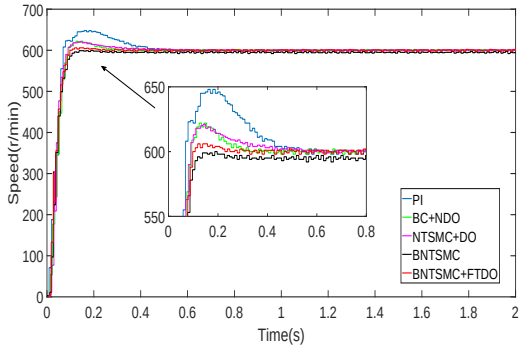

(b)

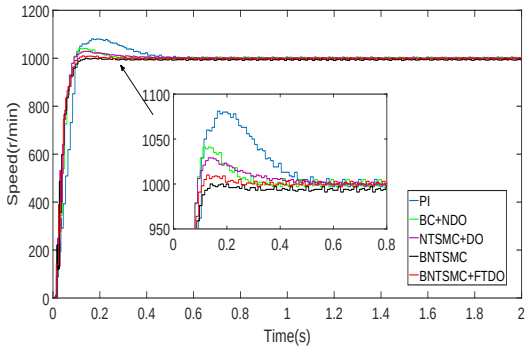

(c)

FIGURE 5: Experimental curves at different speeds: (a) n=200r/min (b) n=600r/min (c) n=1000r/min.

In order to further verify the anti-load disturbance ability of the proposed method, the initial load torque is $0.5N \cdot m$, the load disturbance $1N \cdot m$ and $3N \cdot m$ are imposed to the system at 5s, and removed suddenly from the PMSM at t = 10 s, respectively. The load disturbance curves under three speed conditions are shown in Fig.6-7. Fig.8 shows the electromagnetic torque curve of BNTSMC+FTDO under load disturbance. Fig.9 shows the d_1 disturbance curve estimated by FTDO. It can be seen from the Fig.7 (b) that the speed drop and recovery time of the PI, BC+NDO, NTSMC+DO, and BNTSMC+FTDO methods at 600r/min are 63r, 54r, 55r, 42r and 0.26s, 0.23s, 0.30s, 0.18s, respectively. When the load disturbance is removed, the speed fluctuation and recovery time of these four methods are 60r, 46r, 51r, 42r and 0.24s, 0.23s, 0.42s, 0.19s, respectively. The detailed experimental results at other speeds are shown in Table 2-7. In terms of anti-load disturbance ability, as for BNTSMC control, it cannot attenuate the mismatched disturbance effectively, so it has weak anti-load disturbance ability. The composite control method of BNTSMC+FTDO achieves strong anti-disturbance ability through the compensation of finite-time disturbance observer. Through the analysis of experimental results, the BNTSMC+FTDO method has smaller speed fluctuation and faster response than PI, BC+NDO, BNTSMC, and NTSMC+DO control methods, so the proposed method has the better anti-load disturbance ability.

TABLE 2: Detailed comparison of the three control methods under $1N \cdot m$ load torque disturbance ($n = 200\ r/min$).

Control Scheme	Speed Fluctuation (r/min)		Adjustment Time (s)	
	load up	load down	load up	load down
BNTSMC+FTDO	-20	+13	0.15	0.16
NTSMC+DO	-28	+21	0.22	0.22
BC+NDO	-26	+26	0.17	0.19
PI	-29	+24	0.23	0.22

TABLE 3: Detailed comparison of the three control methods under $1N \cdot m$ load torque disturbance ($n = 600\ r/min$).

Control Scheme	Speed Fluctuation (r/min)		Adjustment Time (s)	
	load up	load down	load up	load down
BNTSMC+FTDO	-13	+13	0.12	0.16
NTSMC+DO	-23	+20	0.28	0.31
BC+NDO	-21	+19	0.18	0.21
PI	-21	+19	0.24	0.23

TABLE 4: Detailed comparison of the three control methods under $1N \cdot m$ load torque disturbance ($n = 1000\ r/min$).

Control Scheme	Speed Fluctuation (r/min)		Adjustment Time (s)	
	load up	load down	load up	load down
BNTSMC+FTDO	-15	+11	0.15	0.18
NTSMC+DO	-24	+29	0.30	0.35
BC+NDO	-19	+16	0.21	0.21
PI	-24	+20	0.24	0.23

TABLE 5: Detailed comparison of the three control methods under $3N \cdot m$ load torque disturbance ($n = 200\ r/min$).

Control Scheme	Speed Fluctuation (r/min)		Adjustment Time (s)	
	load up	load down	load up	load down
BNTSMC+FTDO	-34	+38	0.19	0.20
NTSMC+DO	-53	+50	0.25	0.25
BC+NDO	-54	+46	0.22	0.23
PI	-59	+63	0.27	0.26

This work is licensed under a Creative Commons Attribution-NonCommercial-NoDerivatives 4.0 License. For more information, see https://creativecommons.org/licenses/by-nc-nd/4.0/

This article has been accepted for publication in a future issue of this journal, but has not been fully edited. Content may change prior to final publication. Citation information: DOI 10.1109/ACCESS.2021.3117363, IEEE Access

TABLE 6: Detailed comparison of the three control methods under $3N \cdot m$ load torque disturbance ($n = 600\ r/min$).

Control Scheme	Speed Fluctuation (r/min)		Adjustment Time (s)	
	load up	load down	load up	load down
BNTSMC+FTDO	-42	+42	0.18	0.19
NTSMC+DO	-55	+51	0.30	0.42
BC+NDO	-54	+46	0.23	0.23
PI	-63	+60	0.26	0.24

TABLE 7: Detailed comparison of the three control methods under $3N \cdot m$ load torque disturbance ($n = 1000\ r/min$).

Control Scheme	Speed Fluctuation (r/min)		Adjustment Time (s)	
	load up	load down	load up	load down
BNTSMC+FTDO	-43	+39	0.19	0.18
NTSMC+DO	-56	+53	0.23	0.35
BC+NDO	-54	+50	0.22	0.21
PI	-64	+60	0.22	0.23

In order to continue to verify the robustness of the proposed method with parameter variations, the rotor flux and inductance parameters are changed in the experiment, and the experimental results are shown in Fig.10-13. These parameters are increased or decreased by 30%, respectively. The experiment takes 600r/min as an example for discussion. It can be seen from Fig. 5(b) the overshoot and response time of BNTSMC+FTDO are 6r and 0.31s in the case of no parameter variations. Fig.10 shows the speed and dq axes current curve of the BNTSMC+FTDO method with the increased 30% value of rotor flux (Φ). It can be seen that the overshoot and response time of BNTSMC+FTDO are 13r and 0.33s. Similarly, the overshoot and response time are 4r and 0.29s when the rotor flux (Φ) is decreased by 30% as shown in Fig.11. Then, the experiment of inductance parameter variations is carried out, and the experimental results are shown in Fig.12-13. In Fig.12, the overshoot and response time of the BNTSMC+FTDO method are 6r and 0.30s when the inductance is increased by 30%. When the inductance is decreased by 30%, the overshoot and response time of the BNTSMC+FTDO method are 9r and 0.29s as shown in Fig.13. It can be seen from the experimental comparison results that under the condition of parameter variations, there is no significant effect on the speed tracking and the dq axes current curve compared with no parameter variations. Therefore, the BNTSMC+FTDO method has a good ability to resist parameter disturbance. Meanwhile, although FTDO is not added to the d-axes current controller, d-axes current oscillates around zero. The designed controller has good current control performance and strong robustness.

Next, to verify the performance of the proposed method during reversal, the experiments are also carried out, and the experimental results are shown in Fig.14-15. As can be seen in Fig.14, the overshoot of PI and BC+NDO method when speed reversal at -200r/min, -600r/min, -1000r/min are 28r, 50r, 83r and 16r, 26r, 54r, respectively. And the response time are 0.50s, 0.54s, 0.58s and 0.35s, 0.35s, 0.39s, respectively. The overshoot and response time of the BNTSMC+FTDO method are 12r, 6r, 10r and 0.27s, 0.30s, 0.28s, respectively.

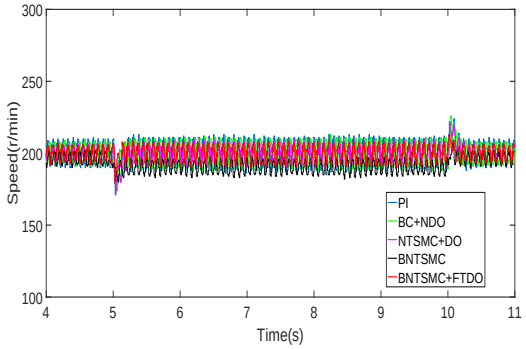

(a)

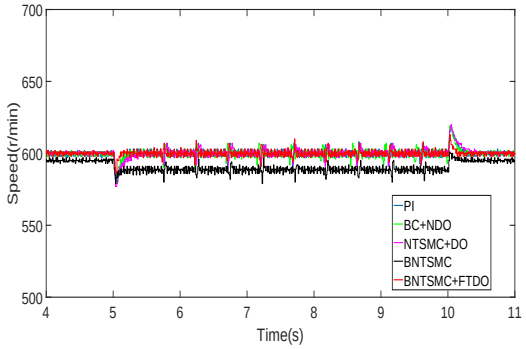

(b)

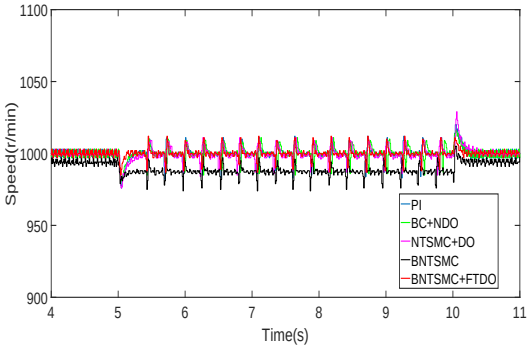

(c)

FIGURE 6: Experimental curves of different speeds under $1N \cdot m$ load disturbance: (a) n=200r/min (b) n=600r/min (c) n=1000r/min.

From the experimental data, it is shown that overshoot and response time of the three methods in the case of reversal are almost the same as the forward rotation. And the BNTSMC+FTDO method has smaller overshoot and shorter response time than the PI and BC+NDO methods. This further illustrates the superiority of the proposed method.

Finally, when the rotation speed is changed suddenly from forward to reverse rotating, the experimental results with three methods are shown in Fig.15. When the speed changes from 200r/min to -200r/min at 5s, the overshoot and response time of BNTSMC+FTDO, BC+NDO and PI methods are

This work is licensed under a Creative Commons Attribution-NonCommercial-NoDerivatives 4.0 License. For more information, see https://creativecommons.org/licenses/by-nc-nd/4.0/

This article has been accepted for publication in a future issue of this journal, but has not been fully edited. Content may change prior to final publication. Citation information: DOI 10.1109/ACCESS.2021.3117363, IEEE Access

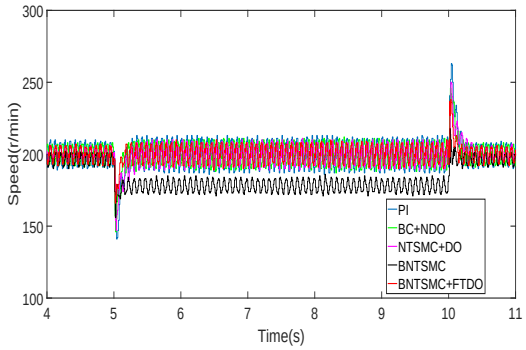

(a)

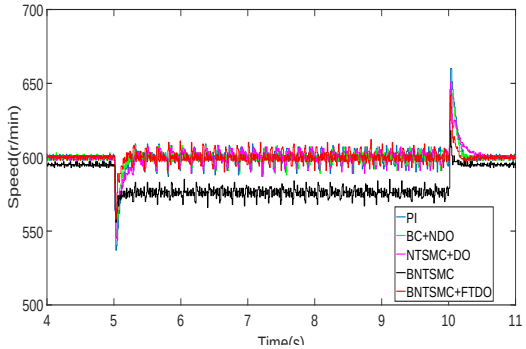

(b)

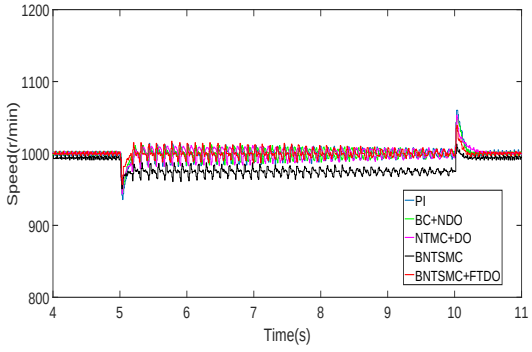

(c)

FIGURE 7: Experimental curves of different speeds under $3N \cdot m$ load disturbance: (a) n=200r/min (b) n=600r/min (c) n=1000r/min.

14r, 19r, 40r and 0.28s, 0.37s, 0.55s, respectively. Similarly, the overshoot and response time of the BNTSMC+FTDO, BC+NDO and PI methods in forward rotation are 8r, 18r, 36r and 0.31s, 0.36s, 0.51s in Fig.15(b). When the speed changes from 400r/min to -400r/min at 5s, the overshoot and response time are 8r, 28r, 64r and 0.30s, 0.37s, 0.59s, respectively. It is shown that BNTSMC+FTDO has smaller overshoot and faster response speed than PI and BC+NDO methods when the speed changes suddenly. When the motor is in the reverse rotation, the overshoot and response time of the BNTSMC+FTDO method are almost the same as the forward rotation. BNTSMC+FTDO method has better dynamic performance even when the speed changes suddenly.

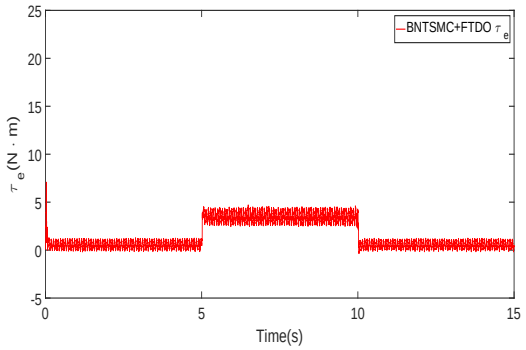

FIGURE 8: Electromagnetic torque curve of BNTSMC+FTDO method under $3N \cdot m$ load disturbance.

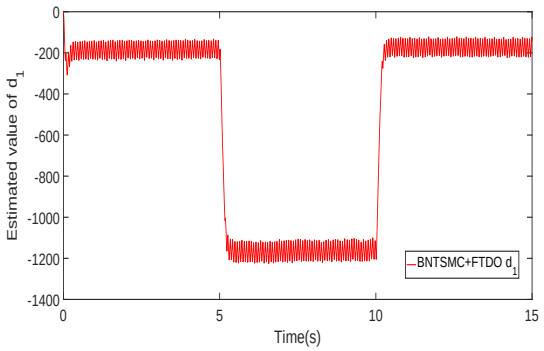

FIGURE 9: The estimated values of d_1.

The experiment proves that the proposed BNTSMC+FTDO method effectively improves the performance of the system. And has the advantages of small overshoot, fast response, strong robustness against parameter variations and external disturbance.

V. CONCLUSION

In this paper, aiming at the speed regulation of permanent magnet synchronous motor, a backstepping nonsingular terminal sliding mode control (BNTSMC) method based on finite time disturbance observer (FTDO) is proposed. First, according to the recursion principle, a backstepping nonsingular terminal sliding mode speed controller based on the Lyapunov function is designed. This method has the asymptotic stability, the finite time convergence and the robustness for the matched disturbance. But for the common sliding mode control, it cannot effectively attenuate the mismatched disturbance. Therefore, in order to further improve the anti-disturbance ability of the system, a finite-time disturbance observer is introduced to estimate the mismatched disturbance in the PMSM system. This compounded control method combines the advantages of the two methods, and it improves the tracking performance, anti-disturbance ability and robustness of the system. The experimental results verify

This work is licensed under a Creative Commons Attribution-NonCommercial-NoDerivatives 4.0 License. For more information, see https://creativecommons.org/licenses/by-nc-nd/4.0/

This article has been accepted for publication in a future issue of this journal, but has not been fully edited. Content may change prior to final publication. Citation information: DOI 10.1109/ACCESS.2021.3117363, IEEE Access

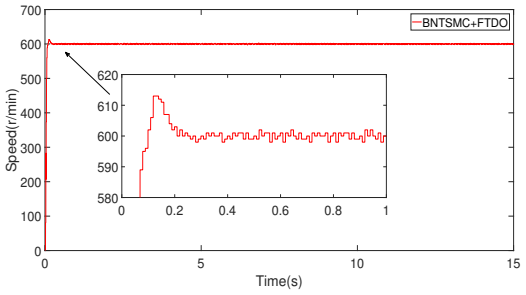

(a)

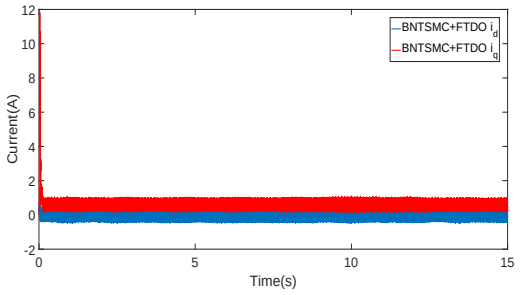

(b)

FIGURE 10: Speed and dq axes current curves of the BNTSMC+FTDO method with the increased 30% value of rotor flux (Φ).

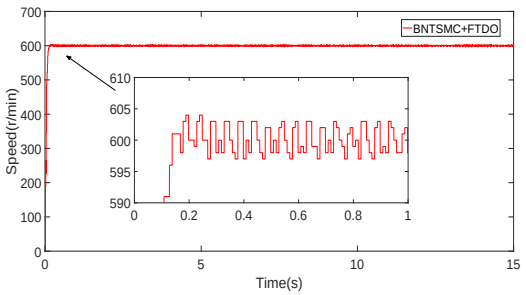

(a)

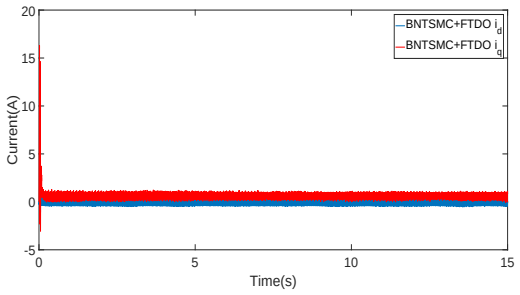

(b)

FIGURE 11: Speed and dq axes current curves of the BNTSMC+FTDO method with the decreased 30% value of rotor flux (Φ).

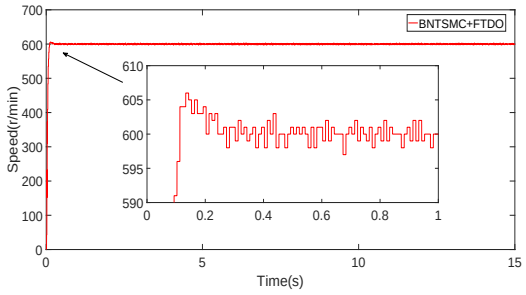

(a)

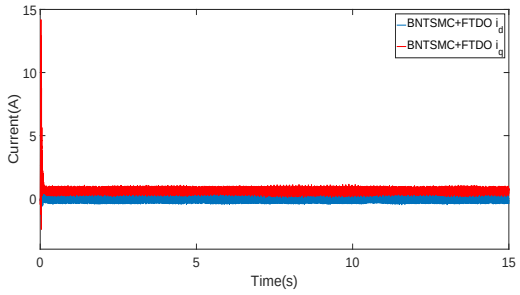

(b)

FIGURE 12: Speed and dq axes current curves of the BNTSMC+FTDO method with the increased 30% value of inductance (L).

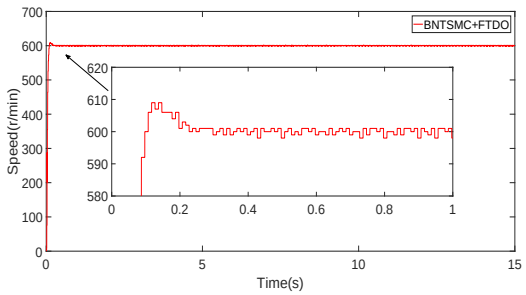

(a)

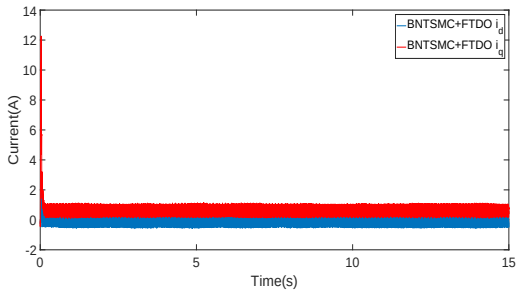

(b)

FIGURE 13: Speed and dq axes current curves of the BNTSMC+FTDO method with the decreased 30% value of inductance (L).

This work is licensed under a Creative Commons Attribution-NonCommercial-NoDerivatives 4.0 License. For more information, see https://creativecommons.org/licenses/by-nc-nd/4.0/

This article has been accepted for publication in a future issue of this journal, but has not been fully edited. Content may change prior to final publication. Citation information: DOI 10.1109/ACCESS.2021.3117363, IEEE Access

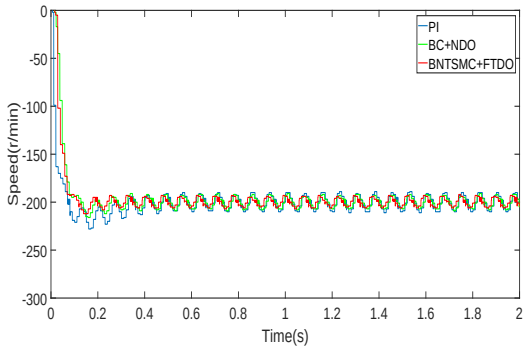

(a)

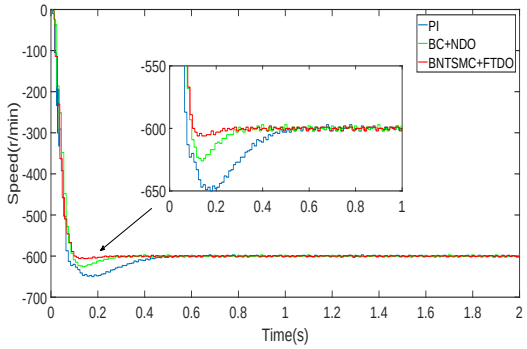

(b)

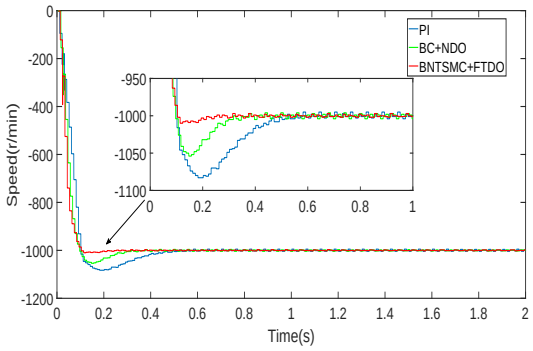

(c)

FIGURE 14: Experimental curves at different speeds: (a) n=-200r/min (b) n=-600r/min (c) n=-1000r/min.

the superiority.

The proposed method in this paper is used the $i_d^* = 0$ control method in the surface permanent magnet synchronous motor. Compared with the $i_d^* = 0$ control of the surface permanent magnet synchronous motor, the MTPA control for the interior permanent magnet synchronous motor can obtain the maximum electromagnetic torque output with smaller stator current. In the future, we will explore the MTPA control for interior permanent magnet synchronous motor.

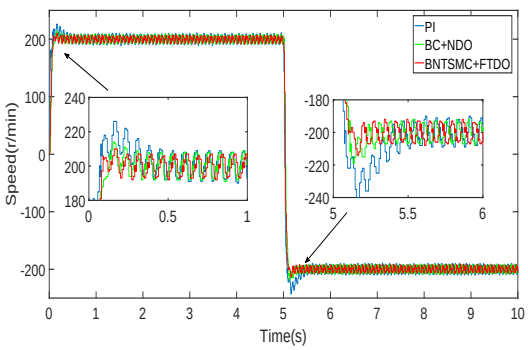

(a)

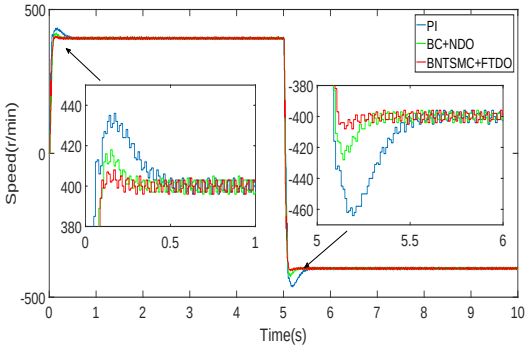

(b)

FIGURE 15: Experimental speed curves when the speed changes suddenly: (a) +200r/min to -200r/min (b) +400r/min to -400r/min.

A. REFERENCES

REFERENCES

[1] B. Cai, Y. Zhao, H. Liu and M. Xie, "Data-Driven Fault Diagnosis Methodology in Three-Phase Inverters for PMSM Drive Systems," IEEE Trans. Power Electron, vol. 32, no. 7, pp. 5590-5600, 2017.

[2] Y. Yan, S. Wang, C. Xia, H. Wang and T. Shi, "Hybrid Control Set-Model Predictive Control for Field-Oriented Control of VSI-PMSM," IEEE Trans. Energy Convers, vol. 31, no. 4, pp. 1622-1633, 2016.

[3] L. Qu, W. Qiao and L. Qu, "An Extended-State-Observer-Based Sliding-Mode Speed Control for Permanent-Magnet Synchronous Motors," IEEE J. Emerg. Sel Topics Power Electron, vol. 9, no. 2, pp. 1605-1613, 2021.

[4] S. Wang, J. Na and Q. Chen, "Adaptive Predefined Performance Sliding Mode Control of Motor Driving Systems With Disturbances," IEEE Trans. Energy Convers, vol. 36, no. 3, pp. 1931-1939, 2021.

[5] Z. Mynar, L. Vesely and P. Vaclavek, "PMSM Model Predictive Control With Field-Weakening Implementation," IEEE Trans. Ind. Electron, vol. 63, no. 8, pp. 5156-5166, 2016.

[6] Wang, Y., Yu, H., Feng, N., Wang, Y, "Non-cascade backstepping sliding mode control with three-order extended state observer for PMSM drive," IET Power Electron, vol. 13, no. 2, pp.307-316, 2020.

[7] H. Sira-Ramírez, J. Linares-Flores and C. García-Rodríguez, "On the control of the permanent magnet synchronous motor: an active disturbance rejection control approach," IEEE Trans. Control Syst. Technol, vol. 22, no. 5, pp. 2056-2063, 2014.

[8] Q. Chen, X. Yu, M. Sun, C. Wu and Z. Fu, "Adaptive Repetitive Learning Control of PMSM Servo Systems with Bounded Nonparametric Uncertainties: Theory and Experiments," IEEE Trans. Ind. Electron, vol. 68, no. 9, pp. 8626-8635, 2021.

[9] S. Barkat, A. Tlemçani, and H. Nouri, "Noninteracting adaptive control of PMSM using interval type-2 fuzzy logic systems," IEEE Trans. Fuzzy Syst, vol. 19, no. 5, pp. 925-936, 2011.

This work is licensed under a Creative Commons Attribution-NonCommercial-NoDerivatives 4.0 License. For more information, see https://creativecommons.org/licenses/by-nc-nd/4.0/

This article has been accepted for publication in a future issue of this journal, but has not been fully edited. Content may change prior to final publication. Citation information: DOI 10.1109/ACCESS.2021.3117363, IEEE Access

[10] M. Krstic, I. Kanellakopoulos, and P.V.Kolotovic, "Nonlinear and Adaptive Control Design," New York, NY, USA: Wiley, 1995.
[11] M. Van, M. Mavrovouniotis and S. Ge, "An adaptive backstepping nonsingular fast terminal sliding mode control for robust fault tolerant control of robot manipulators," IEEE Trans. Syst., Man, Cybern., Syst, vol. 49, no. 7, pp. 1448-1458, 2019.
[12] J. Zhou, Y. Wang, "Adaptive backstepping speed controller design for a permanent magnet synchronous motor," IEE P-Elect. Pow Appl, vol.149, no. 2, pp. 165-172, 2002.
[13] M. Karabacak, H. Eskikurt, "Design, modelling and simulation of a new nonlinear and full adaptive backstepping speed tracking controller for uncertain PMSM," Appl. Math. Model, vol. 36, no. 11, pp. 5199-5213, 2012.
[14] S. Kim, J. Lee and K. Lee, "Offset-free robust adaptive back-stepping speed control for uncertain permanent magnet synchronous motor," IEEE Trans.Power Electron, vol. 31, no.10, pp. 7065-7076, 2016.
[15] G. Schoonhoven, M. Uddin, "MTPA- and FW-Based Robust Nonlinear Speed Control of IPMSM Drive Using Lyapunov Stability Criterion," IEEE Trans. Ind. Appl, vol. 52, no. 5, pp. 4365-4374, 2016.
[16] X. Sun, H. Yu, J. Yu and X. Liu, "Design and implementation of a novel adaptive backstepping control scheme for a PMSM with unknown load torque,"IET Electr. Power Appl, vol. 13, no. 4, pp. 445-455, 2019.
[17] W. Jin, X. Wu and X. Rui, "Adaptive robust backstepping control of the speed regulating differential mechanism for wind turbines," IEEE Trans. Sustain. Energy, vol. 10, no. 3, pp. 1311-1318, 2019.
[18] Y. Ding, E. Kang, S. Wang and G. Chen, "Disturbance suppression for PMSM by a nonlinear composite controller based on two-channel strategy," IET Electr. Power Appl, vol. 14, no. 1, pp. 31-40, 2020.
[19] S. Butt, H. Aschemann, "Adaptive backstepping control for an engine cooling system with guaranteed parameter convergence under mismatched parameter uncertainties," Control Eng. Pract, vol. 64, pp. 195-204, 2017.
[20] J. Yu, P. Shi, W. Dong and B. Chen, "Neural network-based adaptive dynamic surface control for permanent magnet synchronous motors," IEEE Trans. Neural Netw. Learn. Syst, vol. 26, no. 3, pp. 640-645, 2015.
[21] Z. Ma, Z. Liu and P. Huang, "Fractional-order Control for Uncertain Teleoperated Cyber-physical System with Actuator Fault," IEEE/ASME Trans. Mechatronics, doi: 10.1109/TMECH.2020.3039967.
[22] Z. Ma, Z. Liu, P. Huang and Z. Kuang, "Adaptive Fractional Order Sliding Mode Control for Admittance-based Telerobotic System with Optimized Order and Force Estimation," IEEE Trans. Ind. Electron, doi: 10.1109/TIE.2021.3078385.
[23] Z. Ma, P. Huang and Z. Kuang, "Fuzzy Approximate Learning-Based Sliding Mode Control for Deploying Tethered Space Robot," IEEE Trans. Fuzzy Syst, vol. 29, no. 9, pp. 2739-2749, 2021.
[24] F. M. Zaihidee, S. Mekhilef and M. Mubin, "Robust Speed Control of PMSM Using Sliding Mode Control (SMC)- A Review," Energies, vol. 12, no. 9, 2019.
[25] W. Xu, A. K. Junejo, Y. Liu and M. R. Islam, "Improved Continuous Fast Terminal Sliding Mode Control With Extended State Observer for Speed Regulation of PMSM Drive System," IEEE Trans. Veh. Technol, vol. 68, no. 11, 2019.
[26] C. Chiu, "Derivative and integral terminal sliding mode control for a class of MIMO nonlinear systems," Automatica, Vol. 48, pp. 316-326, 2012.
[27] F. M. Zaihidee, S. Mekhilef and M. Mubin, "Application of Fractional Order Sliding Mode Control for Speed Control of Permanent Magnet Synchronous Motor," IEEE Access, vol. 7, pp. 101765-101774, 2019.
[28] J. Davila, "Exact tracking using backstepping control design and high-order sliding modes," IEEE Trans. Autom. Control, vol. 58, no. 8, pp. 2077-2081, 2013.
[29] J. Wu, and Y. Lu, "Adaptive backstepping sliding mode control for boost converter with constant power load," IEEE Access, vol. 7, pp. 50797-50807, 2019.
[30] B. Oubbati, M. Boutoubat, A. Rabhi and M. Belkheir, "Experiential integral backstepping sliding mode controller to achieve the maximum power point of a PV system," Control Eng. Pract, vol. 102, pp. 1-15, 2020.
[31] H. Zhou and Z. Liu, "Vehicle yaw stability-control system design based on sliding mode and backstepping control approach," IEEE Trans. Veh. Technol, vol. 59, no. 7, pp. 3674-3678, 2010.
[32] J. Yang, S. Li, and X. Yu, "Sliding-mode control for systems with mismatched uncertainties via a disturbance observer," IEEE Trans. Ind. Electron, vol. 60, no. 1, pp. 160-169, 2013.
[33] X. Liu, H. Yu, J. Yu, and L. Zhao, "Combined speed and current terminal sliding mode control with nonlinear disturbance observer for PMSM drive," IEEE Access, vol. 6, pp. 29594-29601, 2018.
[34] L. Qiao and W. Zhang, "Trajectory Tracking Control of AUVs via Adaptive Fast Nonsingular Integral Terminal Sliding Mode Control," IEEE Trans. Ind. Informat, vol. 16, no. 2, pp. 1248-1258, 2020.
[35] L. Qiao and W. Zhang, "Double-Loop Integral Terminal Sliding Mode Tracking Control for UUVs With Adaptive Dynamic Compensation of Uncertainties and Disturbances," IEEE J. Ocean. Eng, vol. 44, no. 1, pp. 29-53, 2019.
[36] L. Qiao and W. Zhang, "Adaptive non-singular integral terminal sliding mode tracking control for autonomous underwater vehicles," IET Control Theory Appl, vol. 11, no. 8, pp. 1293-1306, 2017.
[37] Y. Feng, F. Han, and X. Yu, "Chattering free full-order sliding-mode control," Automatica, vol. 50, no. 4, pp. 1310-1314, 2014.
[38] W. Chen, J. Yang, L. Guo and S. Li, "Disturbance-observer-based control and related methods-an overview," IEEE Trans. Ind. Electron, vol. 63, no. 2, pp. 1083-1095, 2016.
[39] D. Ginoya, P. Shendge and S. Phadke, "Sliding mode control for mismatched uncertain systems using an extended disturbance observer," IEEE Trans. Ind. Electron, vol. 61, no. 4, pp. 1983-1992, 2014.
[40] C. Liu, G. Liu and J. Fang, "Feedback linearization and extended state observer-based control for rotor-AMBs system with mismatched uncertainties," IEEE Trans. Ind. Electron, vol. 64, no. 2, pp. 1313-1322, 2017.
[41] A. Chalanga, S. Kamal, L. Fridman and B. Bandyopadhyay, "Implementation of Super-Twisting Control: Super-Twisting and Higher Order Sliding-Mode Observer-Based Approaches," IEEE Trans. Ind. Electron, vol. 63, no. 6, pp. 3677-3685, 2016.
[42] J. Wang, S. Li, J. Yang, B. Wu and Q. Li, "Finite-time disturbance observer based non-singular terminal sliding-mode control for pulse width modulation based DC-DC buck converters with mismatched load disturbances," IET Power Electron, vol. 9, no. 9, pp. 1995-2002, 2016.
[43] J. Linares-Flores, C. García-Rodríguez, and H. Sira-Ramírez, "Robust Backstepping Tracking Controller for Low-Speed PMSM Positioning System: Design, Analysis, and Implementation," IEEE Trans.Ind. Informat, vol. 11, no. 5, pp. 1130-1141, 2015.
[44] Liu, X., Yu, H , "Continuous adaptive integral-type sliding mode control based on disturbance observer for PMSM drives," Nonlinear Dyn, vol. 104, pp. 1429-1441, 2021.
[45] X. Liu, K. Li and C. Zhang, "Improved backstepping control with nonlinear disturbance observer for the speed control of permanent magnet synchronous motor," J. Electr Eng. Technol, vol. 14, no. 1, pp. 275-285, 2019.
[46] G. Prior and M. Krstic, "Quantized-input control lyapunov approach for permanent magnet synchronous motor drives," IEEE Trans. Control Syst. Technol, vol. 21, no. 5, pp. 1784-1794, 2013.
[47] S. A. Q. Mohammed, A. T. Nguyen, H. H. Choi, and J. W. Jung, "Improved iterative learning control strategy for surface-mounted permanent magnet synchronous motor drives," IEEE Trans. Ind. Electron, vol. 67, no. 12, pp. 10134-10144, 2020.
[48] N. Nguyen, H. Oh, Y. Kim, and J. Moon, "Disturbance observer-based continuous finite-time sliding mode control against matched and mismatched disturbances," Complexity, vol. 2020, pp. 1-14, 2020.
[49] J. Wang, S. Li, J. Yang, B. Wu and Q. Li, "Finite-time disturbance observer based non-singular terminal sliding-mode control for pulse width modulation based DC-DC buck converters with mismatched load disturbances," IET Power Electron, vol. 9, no. 9, pp. 1995-2002, 2016.
[50] A. Levant and M. Livne, "Globally convergent differentiators with variable gains," INT J CONTROL, vol. 91, no. 9, pp. 1994–2008, 2018.
[51] Yuri B. Shtessel, Ilya A. Shkolnikov, Arie Levant, "Smooth second-order sliding modes: Missile guidance application," Automatica, vol. 43, no. 8, pp. 1470–1476, 2007

This work is licensed under a Creative Commons Attribution-NonCommercial-NoDerivatives 4.0 License. For more information, see https://creativecommons.org/licenses/by-nc-nd/4.0/

This article has been accepted for publication in a future issue of this journal, but has not been fully edited. Content may change prior to final publication. Citation information: DOI 10.1109/ACCESS.2021.3117363, IEEE Access

TONG LI was born in Shandong, China, in 1996. He received the B.S. degree in automation from Qufu Normal University, Rizhao, China, in 2018, and he is currently pursuing the M.S. degree in Qingdao University, Qingdao, China. His current research interests include power electronics and motor drives.

XUDONG LIU received the B.S. degree and M.S. degree in automation from Qingdao University, Qingdao, China, in 2008 and 2011, respectively, and the Ph.D. degree in power electronics and electric drives from Shandong University, Jinan, China, in 2016. Since 2016, he has been with Qingdao University. His current research interests include new energy system, power electronics and motor drive.

HAISHENG YU received the B.S. degree in electrical automation from the Harbin University of Civil Engineering and Architecture in 1985, the M.S. degree in computer applications from Tsinghua University in 1988, and the Ph.D. degree in control science and engineering from Shandong University, China, in 2006. He is currently a Professor with the School of Automation Engineering, Qingdao University, China. His research interests include electrical energy conversion and motor control, applied nonlinear control, computer control, and intelligent systems.

This work is licensed under a Creative Commons Attribution-NonCommercial-NoDerivatives 4.0 License. For more information, see https://creativecommons.org/licenses/by-nc-nd/4.0/